Tribology International 136 (2019) 446–454

Contents lists available at ScienceDirect

Tribology International

journal homepage: www.elsevier.com/locate/triboint

Atomistic understanding on friction behavior of amorphous carbon films induced by surface hydrogenated modification

Xiaowei Li[a,b,*], Aiying Wang[b], Kwang-Ryeol Lee[a,**]

[a] Computational Science Center, Korea Institute of Science and Technology, Seoul, 136-791, Republic of Korea
[b] Key Laboratory of Marine Materials and Related Technologies, Zhejiang Key Laboratory of Marine Materials and Protective Technologies, Ningbo Institute of Materials Technology and Engineering, Chinese Academy of Sciences, Ningbo, 315201, PR China

ARTICLE INFO

Keywords:
Amorphous carbon
Hydrogenated surface modification
friction property
Reactive molecular dynamics

ABSTRACT

Friction behavior of self-mated amorphous carbon (a-C) films with hydrogenated surface were investigated by reactive molecular dynamics simulation. Results revealed that compared to the hydrogenated a-C (a-C:H) films, hydrogenating the a-C surface only improved the friction property drastically while not deteriorating the intrinsic properties of a-C films. The analysis of interfacial structure demonstrated that being different with a-C:H cases, the competitive relationship between the stress state of H atoms and interfacial passivation caused by H and C-C structural transformation accounted for the evolution of friction coefficient with surface H content. This discloses the friction mechanism of a-C with surface hydrogenated modification and provides an approach to functionalize the carbon-based films with combined tribological and mechanical properties for specific applications.

1. Introduction

Amorphous carbon (a-C) is endowed exceptionally well-supplied physicochemical properties, such as high hardness, low friction coefficient, and corrosion resistance, due to the controllable nanocomposite structure consisted of sp, sp^2, and sp^3 bonding states [1,2]. Especially for hydrogenated a-C (a-C:H) film, the excellent anti-friction property makes it being a strong candidate as solid lubricant for the engineering applications of space-based technologies, automobile engine, and microelectromechanical systems [3,4].

Many efforts also have been conducted to explore the insight into the low friction behavior of a-C films [5–11], and the most popular postulations for the friction mechanism are surface/interface passivation [5–8] and sp^3-to-sp^2 structural transformation [8–11]. For example, Erdemir et al. [5] reported that the elimination of strong covalent and π-π* interactions at the sliding a-C interfaces, combined with the better shielding of carbon atoms by H passivation, resulted in the superlubricity of a-C:H film. Ma et al. [8] studied the friction behavior of a-C:H by molecular dynamics (MD) simulation and revealed that for the film with high H content, a hydrogen-rich monolayer was found at low normal load, functioning as a lubricating transfer layer, while in the film with low H content, the formation of nanocrystalline graphene-like lamellar structure at high normal load, acting as a lubricating agent, contributed to the friction coefficient reduction.

Although a-C:H film is capable of providing a near-frictionless lubrication state under dry sliding condition [12,13] and the above-mentioned results [5,8] also clearly suggest that hydrogen in a-C:H films plays significant improvement in friction reduction, introducing H into a-C film unexpectedly raises the risk of weakening the intrinsic hardness of a-C film [1,5], which cannot satisfy the demands for the combined properties of a-C film in practical application. According to the H-induced passivation mechanism for low friction, is it possible to only functionalize the a-C surface via H for achieving the anti-friction capability while not deteriorating the intrinsic nature of a-C film? Bai et al. [14] investigated the H-terminated a-C films by molecular simulation and found that the existence of antibonding interaction and large repulsive forces on the interface resulted in lower friction coefficient than that of carbon surface model, which was in accordance to the a-C:H cases. Gao et al. [15] also revealed lower friction coefficient of a-C with surface hydrogen than that of H-free case. However, the effect of H-induced surface passivation degrees on the structural properties of friction interface is still not fully elucidated yet, which cannot be collected from previous a-C:H films. In addition, its dependence on contact pressure, which may induce the tribochemical reactions and restructuring of friction interface, is also lacked. This is requisite to provide the scientific understanding on the friction behavior and also

** Corresponding author.
* Corresponding author. Computational Science Center, Korea Institute of Science and Technology, Seoul, 136-791, Republic of Korea.
E-mail addresses: lixw0826@gmail.com (X. Li), krlee@kist.re.kr (K.-R. Lee).

https://doi.org/10.1016/j.triboint.2019.04.019
Received 7 March 2019; Received in revised form 3 April 2019; Accepted 8 April 2019
Available online 11 April 2019
0301-679X/

realize the modulation of a-C surface with effective technique application.

In the present work, by reactive MD (RMD) simulation using ReaxFF force field, we investigated the atomistic friction behaviors of self-mated a-C with hydrogenated surface (a-C@H), the contact pressure was changed to control the contacting state between the self-mated a-C@H surfaces, and the effect of surface H contents on structural properties were systematically analyzed to unveil the underlying friction reduction mechanism. The results exhibited more superior anti-friction in a-C@H film than H-free or oil-lubricated cases, and also demonstrated the complexity and diversity of low friction mechanisms. This finding suggests a new direction to enable an effective manipulation of low friction and the development of new carbon lubricants with robust lubrication properties.

2. Computational details

2.1. Fabrication of H-passivated a-C surface

RMD simulations were conducted to explore the friction process of self-mated a-C@H system using Large-scale Atomic/Molecular Massively Parallel Simulator (LAMMPS) [16]. In order to fabricate the a-C@H film, a multistage strategy was applied [17], as shown in Fig. 1a. The pure a-C structure with size of 42.88 × 40.358 × 34.5 $Å^3$ was set as the substrate, which was composed of 6877 carbon atoms and had the sp^3-C fraction of 24 at.%, sp^2-C fraction of 72 at.%, and density of 2.7 g/cm^3. It was deposited using atom-by-atom method and the detailed deposition process was described elsewhere [18]. Then, in order to hydrogenate the a-C surface, high pressure H_2 gas was introduced as the source of hydrogen and filled the head space of the box, and the number of hydrogen molecules was changed from 100, 400 to 1000 in order to obtain the desired hydrogen content at the a-C surface. After that, the annealing procedure was performed by canonical ensemble employing the Nose-Hoover thermostat [19] with a damping constant 100 fs.

In order to fabricate the H-passivated a-C surface without the deterioration of the intrinsic a-C structure, the effect of different annealing temperatures (1500, 1000, 800, and 600 K) on the density and coordination number distribution were evaluated (see Fig. S1 in Supporting Information), which confirmed 600 K as the optimal annealing temperature. Hence, during the annealing process, the system was first relaxed at 600 K for 125 ps, and then cooled down to 300 K with a cooling rate of 1.2 K/ps. Finally, the a-C@H films (Fig. 1b) were obtained after the additional relaxation at 300 K for 125 ps and the subsequent removing of excess H atoms, and the density and coordination number distributions along the *z* direction (see Fig. S2 in Supporting Information) confirmed that for each case, only the surface region was changed with H_2 content. Table 1 illustrated the hybridized structure of surface region with the thickness of about 13 Å in each a-C@H film. Compared to the pure a-C surface, the increase of surface H content, which ranged from 10.2 at.% to 24.9 at.%, resulted in the reduction of sp- and sp^2-hybridized fractions. In the following study, the structures with different surface H contents were named as a-C@122H, a-C@247H, and a-C@351H, respectively, according to the number of H atoms in each system.

Table 1
Hybridized structure of surface region in obtained a-C@H films.

H atom number	s%	sp%	sp^2%	sp^3%	Name
0	1.8	21.0	60.3	16.9	a-C
122	10.2	11.4	64.6	13.8	a-C@122H
247	18.8	7.0	56.7	17.4	a-C@247H
351	24.9	4.1	50.5	20.5	a-C@351H

2.2. Friction simulation

Fig. 2 showed the friction model in the present calculation. The simulated systems consisted of self-mated a-C@H films with size of 42.88 × 40.358 × 3.5 $Å^3$, in which the number of H atoms changed from 122 to 247 and 351 and the number of C atoms was 6877 (Fig. 1b). The self-mated a-C sliding contact with linear alpha olefin, C_5H_{10}, as lubricating oil [20] or without H [21] were also considered for comparison. The atoms in the outermost thickness of 5 Å along the *z*

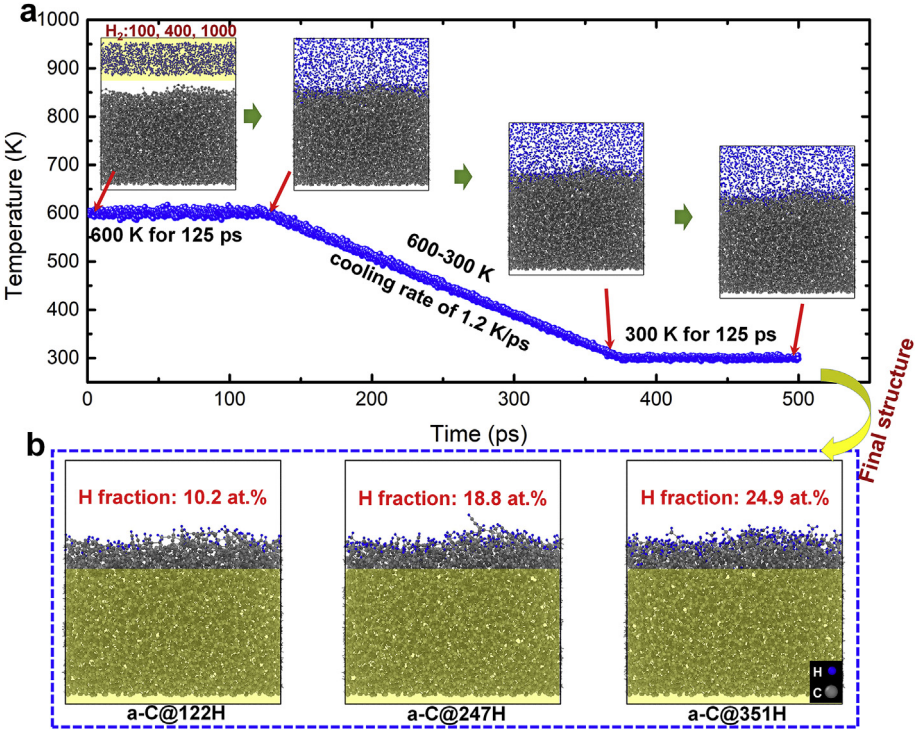

Fig. 1. (a) Fabrication of H-passivated a-C surface by annealing process. (b) Final morphologies of a-C@H films with different surface H contents (inset values).

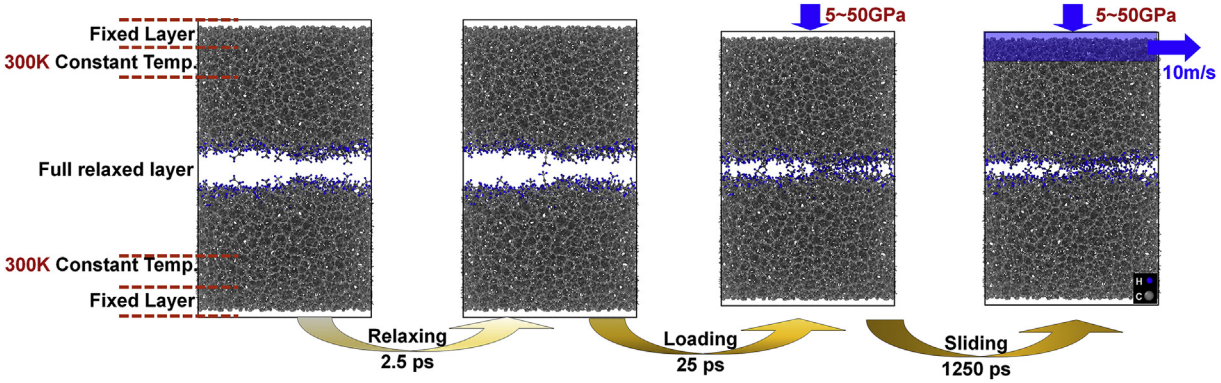

Fig. 2. Friction model of self-mated a-C@H system used in the present calculations and related parameters.

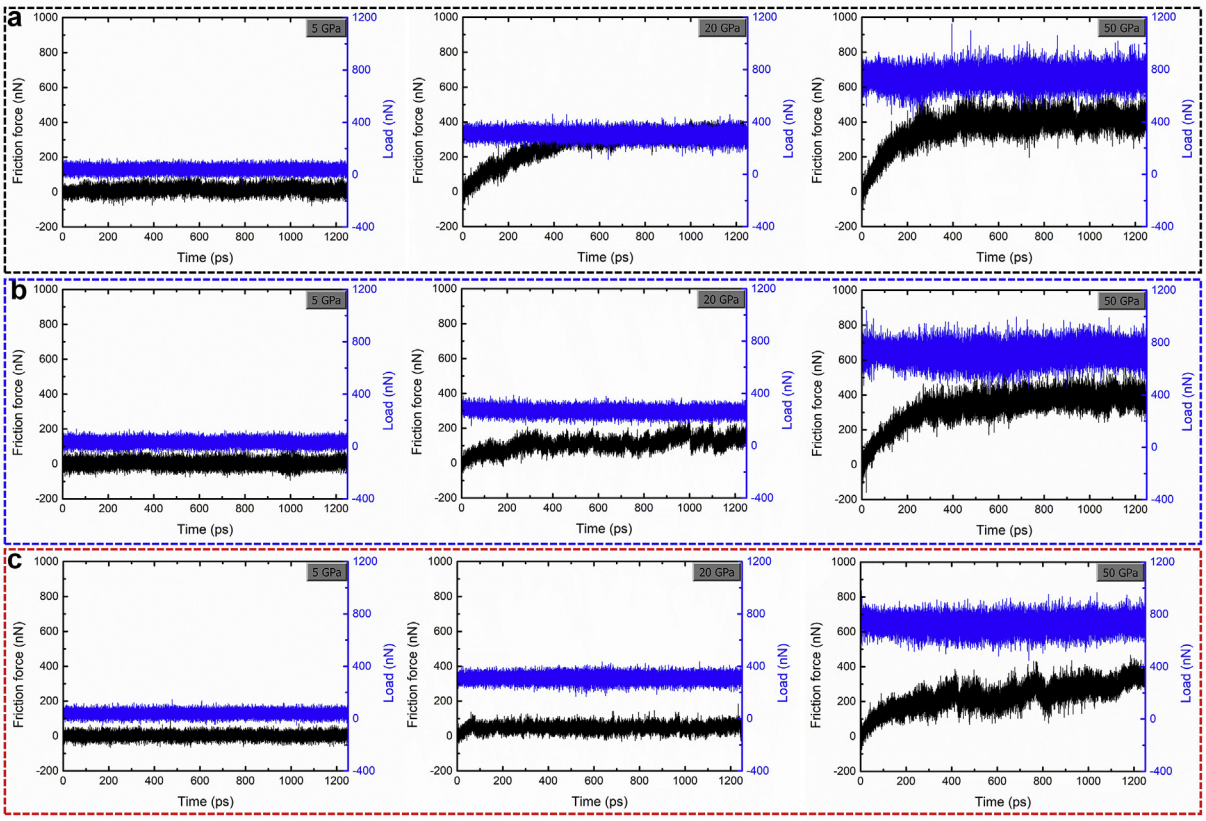

Fig. 3. Friction force and normal force curves as a function of sliding time in self-mated (a) a-C@122H, (b) a-C@247H, and (c) a-C@351H friction systems under different contact pressures.

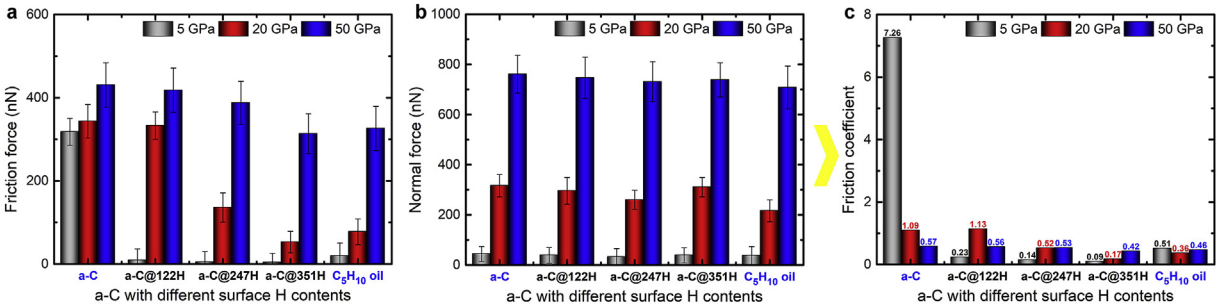

Fig. 4. (a) Average friction force, (b) normal force, and (c) friction coefficient as a function of surface H content for each case. The a-C without H and with C_5H_{10} as lubricating oil are also given for comparison. Errors bars are standard deviations.

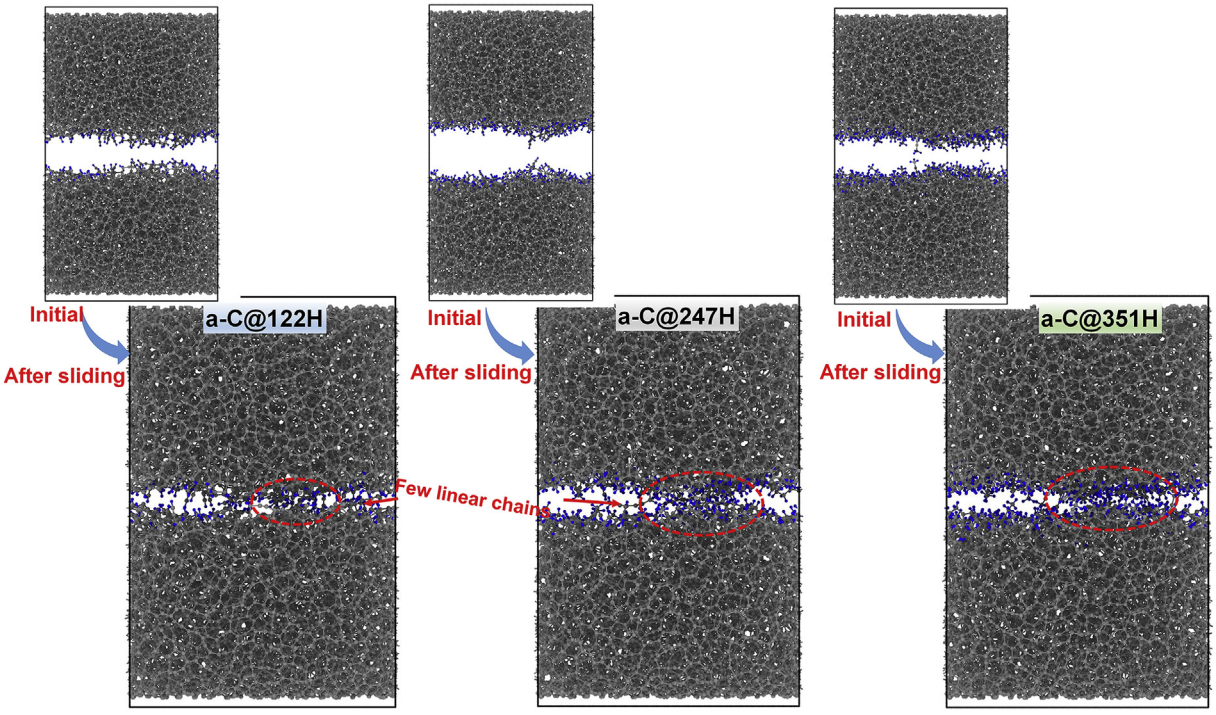

Fig. 5. Initial and final configurations of self-mated a-C@122H, a-C@247H, and a-C@351H friction systems after sliding process under the contact pressure of 5 GPa.

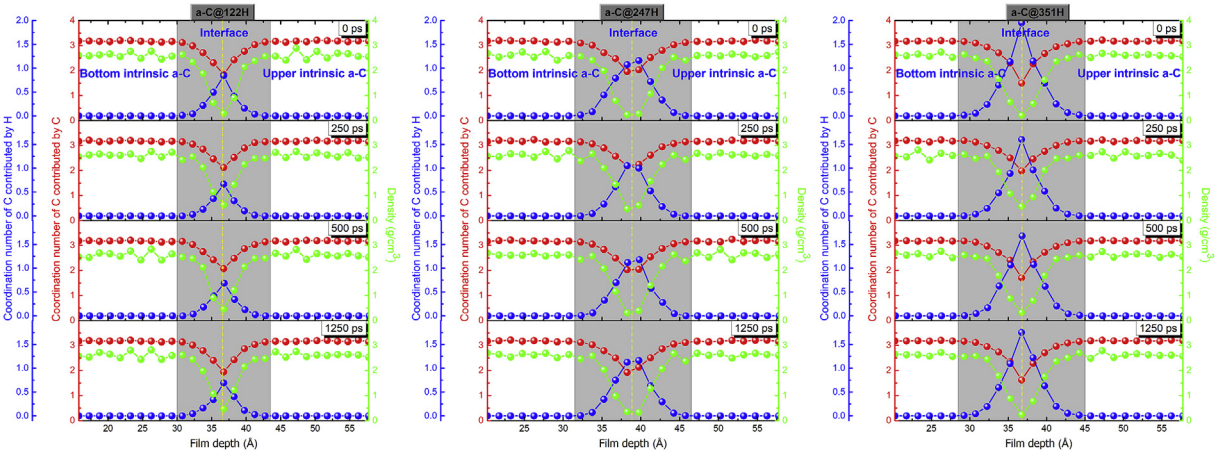

Fig. 6. Coordination numbers per C atom contributed by C and H, respectively, and density profiles along the film depth in self-mated a-C@122H, a-C@247H, and a-C@351H friction systems under the contact pressure of 5 GPa.

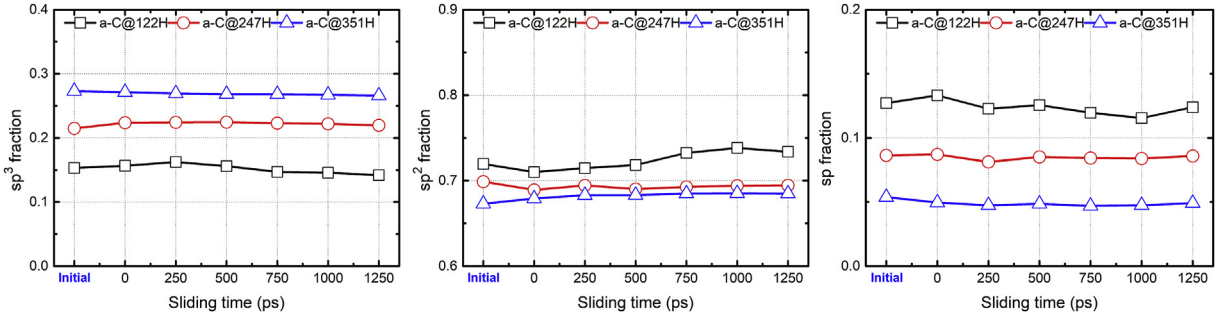

Fig. 7. Hybridized structure (sp^3-C, sp^2-C, and sp-C) of interfaces with sling time in self-mated a-C@122H, a-C@247H, and a-C@351H friction systems under the contact pressure of 5 GPa.

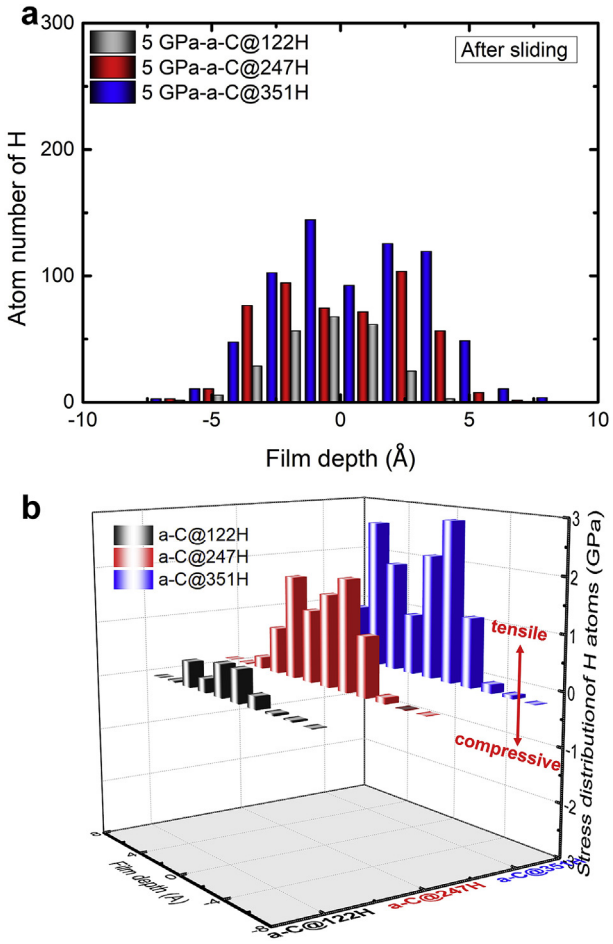

Fig. 8. (a) Atom number and (b) stress distributions of H at friction interface for self-mated a-C@122H, a-C@247H, and a-C@351H friction systems under the contact pressure of 5 GPa after the friction process.

and –*z* directions of each a-C@H film were held rigid; the atoms in the next thickness of 5 Å of both bottom and upper films was coupled to 300 K [22]; all remaining atoms had no constraints placed on them. The initial distance between the bottom and upper mating systems was 3 Å. Before the friction process, the system was first relaxed at 300 K for 2.5 ps, and then the external pressure was applied to the top rigid layer during 25 ps to reach the desired values of 5, 20, or 50 GPa. The high contact pressure, which may be much higher than that from experiments, could be possible for instantaneous contact of a-C asperities during friction process [23]. Our [20,21,24] and previous studies [11,25,26] also confirmed that it was appropriate for examining the friction behavior on an atomic scale. Especially, it should be noted that the direct and accurate comparison between macro- and microscopic results (contact pressure and normal force) was still a big challenge due to the complicated surface state of a-C films including hybridization, adatom passivation, and roughness. After that, due to the limitation of short MD calculation time scale and the requirement for long sliding distance to effectively sample structure [14,27,28], the constant velocity of 10 m/s along the *x* direction was exerted to the upper rigid layer to slide the system under a fixed pressure, and the sliding process lasted 1.25 ns to get the steady-state friction stage.

During the annealing and friction process, the periodic boundary conditions were applied along both the *x* and *y* directions, and a MD timestep of 0.25 fs was used. ReaxFF [29,30] was used to describe the C-C, C-H, and H-H interactions. It is a reactive force field and uses the bond order concept to consider the instantaneous interaction between the atoms, allowing for the formation and dissociation of covalent bond and the chemical reactions in complicated carbon-based systems, with high accuracy comparable to quantum calculations. The reliability of the used force field to our present calculations has been also validated adequately by our RMD and ab-initio calculations [20,21,24].

3. Results and discussion

Fig. 3 shows the friction force and normal force curves as a function of sliding time to evaluate the effect of surface passivation degree on the friction properties of a-C films under different contact pressures, in which the forces acting on the fixed atoms of bottom a-C layer in the *x* and *z* directions are summed for each time step, respectively, as the friction force and normal force values [20,21,24,26]. It reveals that for each case, the friction force increases first and then becomes stable until the end of the sliding process, but the evolutions of friction force and normal force with sliding time are strongly related with the surface H content and contact pressure. When the systems work under a fixed contact pressure, the friction force and normal force with surface H content quickly reach the steady-state friction stage, which are followed by the weakened fluctuations [8]. However, for a fixed friction system, when the contact pressure ranges from 5 to 50 GPa, the time taken for running-in process increases obviously following the enhanced fluctuations of friction force and normal force. This suggests the significant interaction at the friction interface. The similar changes in temperature, kinetic energy, and potential energy to that of friction force are also observed, as illustrated in Fig. S3 of Supporting Information. In order to quantify the effect of different surface H contents on the friction behaviors, the values from the last 200 ps in Fig. 3 are adopted to calculate the average friction force and normal force at the steady-state friction stage.

The variations in the average friction force and normal force as a function of surface H content are illustrated in Fig. 4a and b, respectively, for each case. For comparison, the a-C friction cases without H passivation [21] and with linear olefin C_5H_{10} as a lubricating oil [20] are also considered. It can be seen that with increasing the surface H content, the friction force decreases monotonously for each contact pressure and the system with high H content favors the low friction force (Fig. 4a), demonstrating the key role of H in reducing the friction [14,15], while the average normal force values in Fig. 4b have slight change due to the similar surface roughness of a-C@H films (see Fig. S4 of Supporting Information). In addition, for the same friction system, both the friction force and normal force with contact pressure increase, but different increasing rates are displayed, leading to the distinct friction response on contact pressure, which is similar to Li's report [20]. According to the average values of friction force (Fig. 4a) and normal force (Fig. 4b), the friction coefficient is calculated, as shown in Fig. 4c. It reveals that the friction coefficient as a function of surface H content decreases, agreeing well with the a-C:H cases [8], but compared to those under 5 and 20 GPa, it only has a slight decrease when the contact pressure is 50 GPa, indicating the significant structural transformation induced by contact pressure [20]. The minimal friction coefficient of 0.09 is obtained for a-C@351H friction system under 5 GPa, which is much lower than the a-C:H films [8].

Furthermore, by comparison with the H-free case [21], it proves that the surface hydrogenated modification could improve the friction property obviously, especially under the low contact pressure condition, and the lubricating efficiency is further promoted by increasing the surface H content. Interestingly, compared to the C_5H_{10}-lubricated case [20], the surface hydrogenated modification also shows the potential to realize better friction property than fluid lubrication, although it can be improved to a large extent by changing the fluid viscosity and friction conditions; even under the extreme contact pressure of 50 GPa, the more excellent friction property can also be achieved by raising the surface H content. This suggests an effective approach to capture the high-efficiency lubrication by surface-passivated modification instead of the addition of lubricating oil.

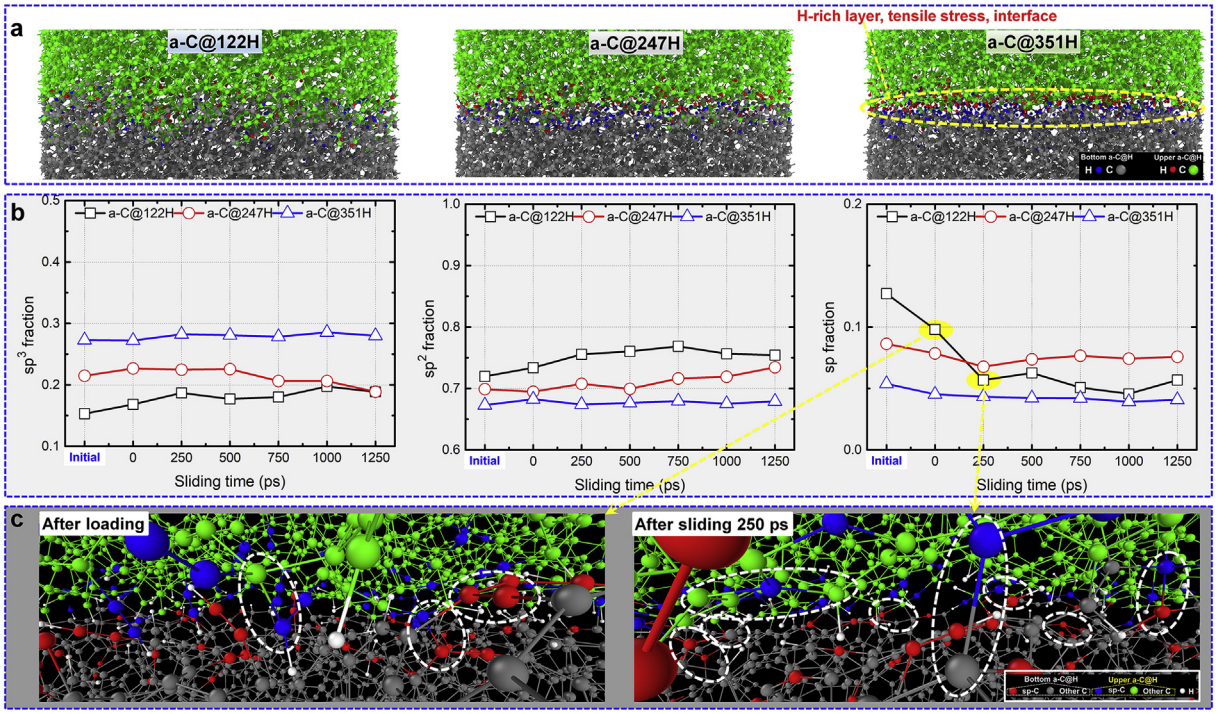

Fig. 9. (a) Snapshots of friction interfaces after sliding process, (b) hybridized structure (sp^3-C, sp^2-C, and sp-C) of interfaces with sling time in self-mated a-C@122H, a-C@247H, and a-C@351H friction systems under the contact pressure of 20 GPa. (c) Local configurations of friction interface in self-mated a-C@122H when the sliding time is 0 and 250 ps, respectively.

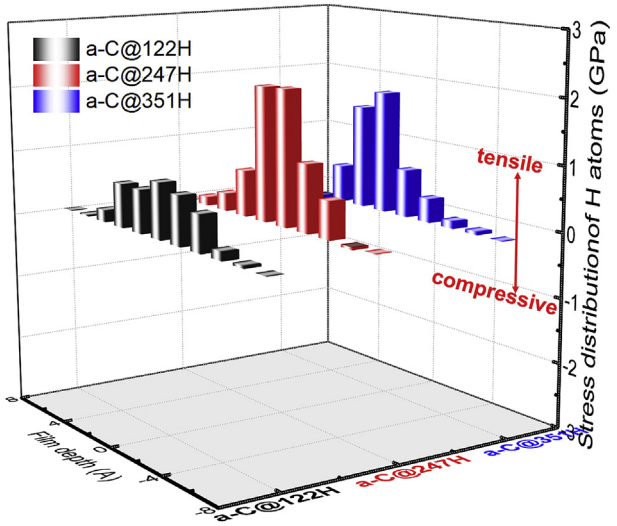

Fig. 10. Stress distributions of H at friction interface for self-mated a-C@122H, a-C@247H, and a-C@351H friction systems under the contact pressure of 20 GPa after friction process.

In order to explore the underlying friction mechanism caused by different surface H contents, the structural transformation of friction interface, which is strongly related with the friction behavior, needs to be analyzed. Fig. 5 gives the atomic snapshots of self-mated a-C@122H, a-C@247H, and a-C@351H friction systems in the *x*-*z* plane when the contact pressure is fixed at 5 GPa. Compared to the initial cases, the friction interface can be distinguished clearly after the friction process when the contact pressure is 5 GPa, at which the direct interaction between the bottom and upper contacting structures can be prevented by the repulsion force of surface H atoms [14]. There are a few C-C linear chains existed at the interface. Especially, note that during the friction process, H atoms could effectively passivate the bulges or sites with high asperities (red circles in Fig. 5) at the surface for each case, which could furtherly diminish the effect of C-C bonding interaction on friction.

Before characterizing the interfacial structure, the coordination number and density profile along the film depth are analyzed first for each case to define the width of interfacial region, as shown in Fig. 6. The widths of interfacial region (gay color in Fig. 6) are 13.5 Å for a-C@122H, 15 Å for a-C@247H, and 16.5 Å for a-C@351H, respectively. Based on the specified interfacial regions, Fig. 7 shows the change in carbon hybridized structure of interface with sliding time for each case under the contact pressure of 5 GPa. Compared to the initial structure, the carbon hybridized structure almost has no variation for each case during the sliding process, indicating that the a-C surface is chemically stable and passivated by H, and the friction behavior under 5 GPa should be mainly dominated by the H atoms.

On the one hand, increasing the H content could further passivate the a-C surface, as shown in Fig. 7. On the other hand, Fig. 8a shows that H atoms mainly distribute at the friction interface to separate the contacting films completely, which is also confirmed by Fig. 5, and most importantly, they exhibit the tensile stress state (Fig. 8b), corresponding to the strong repulsive force [14] and thus leading to the easy slippage of friction interface. Hence, when the contact pressure is 5 GPa, the improved interfacial passivation and repulsive force, which are induced by H atoms, give explanation for the significant reduction of friction coefficient with surface H content (from 0.23 to 0.14 and 0.09), as shown in Fig. 4.

As the contact pressure increases to 20 from 5 GPa, different structure transformations happen for each case (Fig. 9a). For the self-mated a-C@122H system, it shows the obvious intermixing of C and H atoms from both the mating films, implying the presence of the chemical interaction and rehybridization of friction interface. However, in self-mated a-C@247H and a-C@351H friction systems, the H atoms originated from the bottom and upper sliding films adhere to the interface significantly, generating a stable and dense hydrogen-rich layer to highly passivate the sliding interface (Fig. 9a), which may act as lubricating agent for low friction behavior and also hinder the

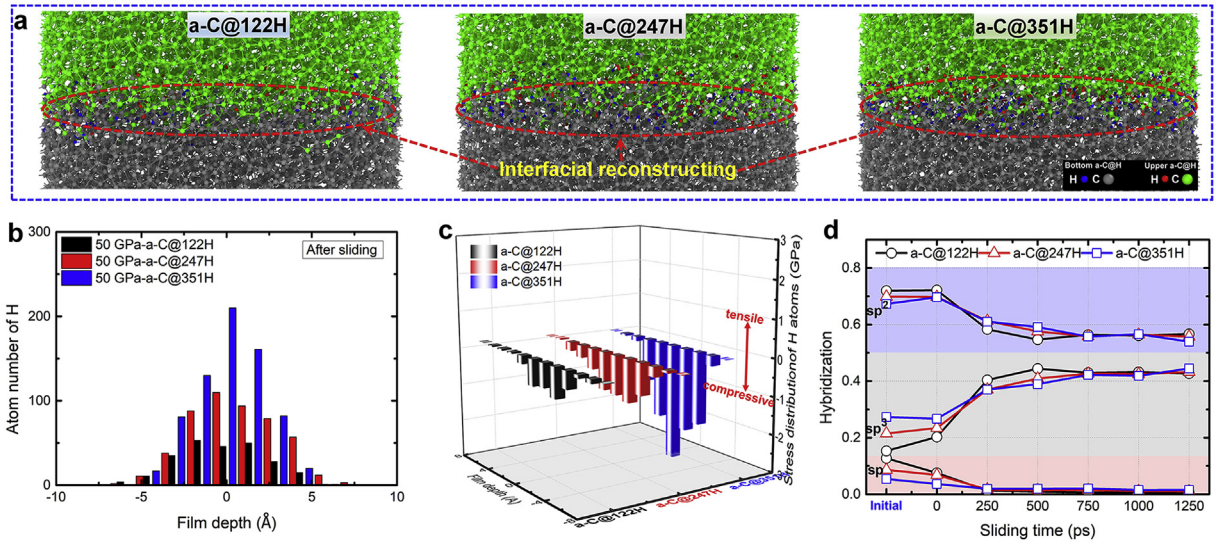

Fig. 11. (a) Snapshots of friction interfaces after sliding process, (b) Atom number distribution of H, (c) Stress distributions of H, and (d) hybridized structure (sp^3-C, sp^2-C, and sp-C) of interface with sliding time in self-mated a-C@122H, a-C@247H, and a-C@351H friction systems under the contact pressure of 50 GPa.

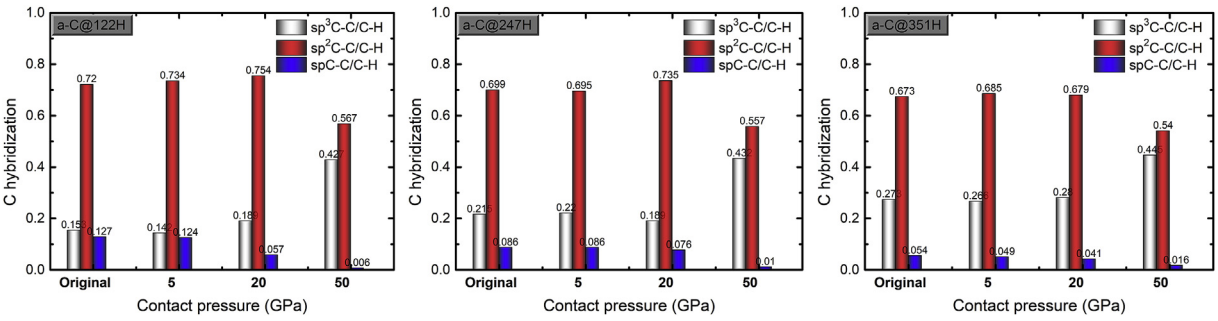

Fig. 12. Hybridized structure (sp^3-C, sp^2-C, and sp-C) of friction interfaces as a function of contact pressure in self-mated a-C@122H, a-C@247H, and a-C@351H friction systems, respectively.

deformation and structural transformation of interface [8]. This is also proved by the evolution of hybridized structure during the sliding process, as given in Fig. 9b.

However, for self-mated a-C@122H system with low H content, there is an obvious change in the hybridized structure of interface (Fig. 9b). In particular, the sp-C fraction shows a significant reduction following the increased sp^2-C and sp^3-C fractions, which mainly occurs during the sliding time from 0 to 250 ps. By analyzing the corresponding local configurations at 0 and 250 ps separately (Fig. 9c), it reveals that due to the low H content, the unsaturated sp-C atoms could serve as initiation points for chemical reactions and bond with the C atoms from both surfaces to form the sp^2-and sp^3-hybridized states. Among of them, the interfilm C-C bonding between the two counterfaces is also generated in self-mated a-C@122H system, which will enhance the adhesion between the two counterfaces and thus prevent the shearing process [15], but this behavior is suppressed by the formed hydrogen-rich layer at the interface of a-C@247H and a-C@351 systems.

Moreover, the stress of H atoms also shows the tensile state for each case and it increases with surface H content (Fig. 10), although they are smaller than those under 5 GPa (Fig. 8b). Combined with the decreased interfilm interaction, the differences in stress and interfacial passivation caused by H atoms contribute to the friction behavior with surface H content under 20 GPa. In addition, there is no layered graphitic structure formed for the a-C@122H system, being different with those in the diamond/a-C:H [8] or diamond/a-C friction systems [11]. This indicates that the friction behavior is also strongly dependent on the mating materials, and the one with regular crystal structure, such as diamond, may favor the formation of layered graphitic structure, and this also implies the difference in underlying friction mechanism.

With further increasing the contact pressure up to 50 GPa, the tribochemical reactions occur drastically at the interface for each case following the interfacial reconstruction and the formation of intermixing interface between the bottom and upper mating films, as shown in Fig. 11a. Due to the interdiffusion and migration of H atoms into intrinsic a-C structures (Fig. 11b), the stress of H atoms evolves from tensile to compressive state (Fig. 11c), suggesting the attractive force, which is not favorable for the sliding of friction interface, and the attractive force also increases with surface H content. However, the friction coefficient with surface H content shows a slight decrease (Fig. 4). This indicates that the stress state of H atoms does not dominate the friction behavior of a-C@H system under 50 GPa. Instead, the interfacial passivation, which originates from the H-induced passivation and C-C structural transformation, plays an essential role in the present contact pressure for each case. This is similar to the results reported by Cui et al. [31].

Fig. 11d illustrates the carbon hybridized structure as a function of sliding time for each system under 50 GPa. It reveals that except the H-induced passivation, the high pressure-induced structural transformation, especially the sp^2-to-sp^3 and sp-to-sp^3 rehybridizations [20,21], further passivates the friction interface, dominating the sliding process for each case, which is mentioned but not given with the evidence in previous report [8]. In addition, this structural transformation is inspired by the evolution of residual stress, in which high compressive

stress favors the formation of sp^3 structure according to *P-T* phase diagram for carbon [11,32].

Furthermore, it should be mentioned that the friction behavior is also highly dependent on the contact pressure, and Fig. 4 also indicates that for each friction system, the friction coefficient as a function of contact pressure exhibits different evolutions. For a-C@122H, the friction coefficient increases first and then decreases, while a linear increase for friction coefficient is observed for a-C@351H system. This is in accordance with previous calculation [8,15] and experimental studies [33]. When the contact pressure changes from 5 to 20 GPa, there is no obvious change in interfacial structure except for self-mated a-C@122H (Fig. 12), and thus the increased friction coefficient mainly attributes to the decrease of repulsive force caused by H (Figs. 8b and 10) and the existence of interfilm interaction (Fig. 9c). With the contact pressure reaching up to 50 GPa, the repulsive force of H atoms transforms to the attractive state (Fig. 11c), but it can be compensated by the highly interfacial passivation in self-mated a-C@122H (Fig. 11d), causing the reduction of friction coefficient; for self-mated a-C@247H system, the attractive force of H atoms at 50 GPa is higher than that in self-mated a-C@122H system, so the interfacial passivation neutralizes the attractive force, inducing no change in friction coefficient; however, for self-mated a-C@351 system, the highest attractive force (Fig. 11c), which cannot be compensated by the interface passivation of dangling bonds, aggravates the friction coefficient.

4. Conclusions

In this study, RMD simulation was carried out to study the dependence of friction property of a-C@H on surface H content under different contact pressures, and the interfacial structure was mainly analyzed to clarify the underlying friction mechanism. Results revealed that.

(1) When the annealing temperature was less than 600 K, the hydrogenated treatment on a-C films only passivated the surface structure while not deteriorated the intrinsic mechanical properties of a-C film.
(2) For the self-mated a-C@H friction system, the friction property was strongly dependent on the surface H content and contact pressure. Among the loading range from 5 to 20 GPa, the H atoms mainly distributed at the interface, prohibiting the structural transformation, and gave the repulsive force to separate the friction interface; increasing the surface H content could enhance the repulsive force and interfacial passivation following the reduction of friction coefficient. However, when the contact pressure was 50 GPa, although the H atoms exhibited the attractive force instead of repulsive force, the friction interface was highly reconstructed and passivated by the sp-to-sp^3 and sp^2-to-sp^3 structural transformations, which mainly dominated the friction process.
(3) In particular, compared to the H-free and oil-lubricated cases, the hydrogenated modification of a-C surface exhibited better anti-friction property with raising the H content. Although the a-C@H films are not the representative of a-C films generated in experiment, it is also still a big challenge for the direct comparison between the simulation and experimental results. This is due to the limitations in the simplified contact model, friction parameters, the hybridized structure and surface state of a-C observed in experiment. But these present simulations do provide insight into the potential tribochemical reaction and fundamental friction mechanism caused by surface hydrogenated modification, and also suggest an effective approach to realize the high-efficiency lubrication through the surface-passivated modification instead of oil-based lubrication and the H-doped a-C intrinsic structure.

Acknowledgments

This research was supported by the Korea Research Fellowship Program funded by the Ministry of Science and ICT through the National Research Foundation of Korea (2017H1D3A1A01055070), the Nano Materials Research Program through the Ministry of Science and IT Technology (NRF-2016M3A7B4025402), the National Natural Science Foundation of China (51772307), and Zhejiang Key Research and Development Program (2017C01001).

Appendix A. Supplementary data

Supplementary data related to this article can be found at https://doi.org/10.1016/j.triboint.2019.04.019.

References

[1] Robertson J. Diamond-like amorphous carbon. Mater Sci Eng R Rep 2002;37:129–281.
[2] Wang Y, Gao K, Zhang B, Wang Q, Zhang J. Structure effects of sp^2-rich carbon films under super-low friction contact. Carbon 2018;137:49–56.
[3] Mustafa MMB, Umehara N, Tokoroyama T, Murashima M, Shibata A, Utsumi Y, Moriguchi H. Effect of mesh structure of tetrahedral amorphous carbon (ta-C) coating on friction and wear properties under base-oil lubrication condition. Tribol Int 2019. https://doi.org/10.1016/j.triboint.2019.01.016.
[4] Wan S, Li D, Zhang G, Tieu AK, Zhang B. Comparison of the scuffing behavior and wear resistance of candidate engineered coatings for automotive piston rings. Tribol Int 2017;106:10–22.
[5] Erdemir A. The role of hydrogen in tribological properties of diamond-like carbon films. Surf Coating Technol 2001;146–147:292–7.
[6] Eryilmaz OL, Erdemir A. On the hydrogen lubrication mechanism(s) of DLC films: an imaging TOF-SIMS study. Surf Coating Technol 2008;203:750–5.
[7] Konicek AR, Grierson DS, Sumant AV, Friedmann TA, Sullivan JP, Gilbert PUPA, Sawyer WG, Carpick RW. Influence of surface passivation on the friction and wear behavior of ultrananocrystalline diamond and tetrahedral amorphous carbon thin films. Phys Rev B 2012;85:155448.
[8] Chen YN, Ma TB, Chen Z, Hu YZ, Wang H. Combined effects of structural transformation and hydrogen passivation on the friction behaviors of hydrogenated amorphous carbon films. J Phys Chem C 2015;119:16148–55.
[9] Liu Y, Erdemir A, Meletis EI. An investigation of the relationship between graphitization and frictional behavior of DLC coatings. Surf Coating Technol 1996;86–87:564–8.
[10] Liu Y, Meletis EI. Evidence of graphitization of diamond-like carbon films during sliding wear. J Mater Sci 1997;32:3491–5.
[11] Ma TB, Hu YZ, Wang H. Molecular dynamics simulation of shear-induced graphitization of amorphous carbon films. Carbon 2009;47:1953–7.
[12] Chen X, Zhang C, Kato T, Yang X, Wu S, Wang R, Nosaka M, Luo J. Evolution of tribo-induced interfacial nanostructures governing superlubricity in a-C:H and a-C:H:Si films. Nat Commun 2017;5:1675.
[13] Cui L, Zhou H, Zhang K, Lu Z, Wang X. Bias voltage dependence of superlubricity lifetime of hydrogenated amorphous carbon films in high vacuum. Tribol Int 2018;117:107–11.
[14] Bai S, Onodera T, Nagumo R, Miura R, Suzuki A, Tsuboi H, Hatakeyama N, Takaba H, Kubo M, Miyamoto A. Friction reduction mechanism of hydrogen- and fluorine-terminated diamond-like carbon films investigated by molecular dynamics and quantum chemical calculation. J Phys Chem C 2012;116:12559–65.
[15] Gao GT, Mikulski PT, Chateauneuf GM, Harrison JA. The effects of films structure and surface hydrogen on the properties of amorphous carbon films. J Phys Chem B 2003;107:11082–90.
[16] Plimpton S. Fast parallel algorithms for short-range molecular dynamics. J Comput Phys 1995;117:1–19.
[17] Lotfi R, Jonayat ASM, van Duin ACT, Biswas M, Hempstead R. A reactive force field study on the interaction of lubricant with diamond-like carbon structures. J Phys Chem C 2016;120:27443–51.
[18] Li X, Wang A, Lee KR. Comparison of empirical potentials for calculating structural properties of amorphous carbon films by molecular dynamics simulation. Comput Mater Sci 2018;151:246–54.
[19] Evans DJ, Holian BL. The nose-hoover thermostat. J Chem Phys 1985;83:4069–74.
[20] Li X, Wang A, Lee KR. Mechanism of contact pressure-induced friction at the amorphous carbon/alpha olefin interface. npj Comput Mater 2018;4:53.
[21] Li X, Wang A, Lee KR. Insights on low-friction mechanism of amorphous carbon films from reactive molecular dynamics study. Tribol Int 2019;131:567–78.
[22] Berendsen HJC, Postma JPM, van Gunsteren WF, DiNola A, Haak JR. Molecular dynamics with coupling to an external bath. J Chem Phys 1984;81:3684–90.
[23] Ma TB, Wang LF, Hu YZ, Li X, Wang H. A shear localization mechanism for lubricity of amorphous carbon materials. Sci Rep 2014;4:3662.
[24] Li X, Wang A, Lee KR. Tribo-induced structural transformation and lubricant dissociation at amorphous carbon-alpha olefin interface. Adv Theory Simul 2019;2:1800157.
[25] Kuwahara T, Romero PA, Makowski S, Weihnacht V, Moras G, Moseler M.

Mechano-chemical decomposition of organic friction modifiers with multiple reactive centers induces superlubricity of ta-C. Nat Commun 2019;10:151.
[26] Bai S, Murabayashi H, Kobayashi Y, Higuchi Y, Ozawa N, Adachi K, Martin M, Kubo M. Tight-binding quantum chemical molecular dynamics simulations of the low friction mechanism of fluorine-terminated diamond-like carbon films. RSC Adv 2014;4:33739–48.
[27] Wang Y, Xu J, Ootani Y, Bai S, Higuchi Y, Ozawa N, Adachi K, Martin JM, Kubo M. Tight-binding quantum chemical molecular dynamics study on the friction behavior and wear processes of diamond-like carbon coatings: effect of tensile stress. ACS Appl Mater Interfaces 2017;9:34396–404.
[28] Wang Y, Xu J, Zhang J, Chen Q, Ootani Y, Higuchi Y, Ozawa N, Martin JM, Adachi K, Kubo M. Tribochemical reactions and graphitization of diamond-like carbon against alumina give volcano-type temperature dependence of friction coefficients: a tight-binding quantum chemical molecular dynamics simulation. Carbon 2018;133:350–7.
[29] Srinivasan SG, Van Duin ACT, Ganesh P. Development of a ReaxFF potential for carbon condensed phases and its application to the thermal fragmentation of a large fullerene. J Phys Chem A 2015;119:571–80.
[30] Tavazza F, Senftle TP, Zou C, Becker CA, Van Duin ACT. Molecular dynamics investigation of the effects of tip-substrate interactions during nanoindentation. J Phys Chem C 2015;119:13580–9.
[31] Cui L, Lu Z, Wang L. Probing the low-friction mechanism of diamond-like carbon by varying of sliding velocity and vacuum pressure. Carbon 2014;66:259–66.
[32] McKenzie DR, Muller D, Pailthorpe BA. Compressive-stress induced formation of thin-film tetrahedral amorphous carbon. Phys Rev Lett 1991;67:773–6.
[33] Erdemir A. Genesis of superlow friction and wear in diamondlike carbon films. Tribol Int 2004;37:1005–12.